

Switchable focus using a polymeric lenticular microlens array and a polarization rotator

Hongwen Ren,^{1,*} Su Xu,² Yifan Liu,² and Shin-Tson Wu²

¹Department of polymer Nano-Science and Tech., Chonbuk National University, Jeonju, Jeonbuk, 561-756, South Korea

²CREOL, The College of Optics and Photonics, University of Central Florida, Orlando, Florida 32816, USA
[*hongwen@jbnu.ac.kr](mailto:hongwen@jbnu.ac.kr)

Abstract: We demonstrate a flat polymeric lenticular microlens array using a mixture of rod-like diacrylate monomer and positive dielectric anisotropy nematic liquid crystal (LC). To create gradient refractive index profile in one microlens, we generate fringing fields from a planar top electrode and two striped bottom electrodes. After UV stabilization, the film is optically anisotropic and can stand alone. We then laminate this film on a 90° twisted-nematic LC cell, which works as a dynamic polarization rotator. The static polymeric lenticular lens exhibits focusing effect only to the extraordinary ray, but no optical effect to the ordinary ray. Such an integrated lens system offers several advantages, such as low voltage, fast response time, and temperature insensitivity, and can be used for switchable 2D/3D displays.

©2013 Optical Society of America

OCIS codes: (120.2040) Displays; (160.3710) Liquid crystals; (160.5470) Polymers; (220.3620) Lens system design; (220.2560) Propagating methods.

References and links

1. H. Choi, J.-H. Park, J. Kim, S.-W. Cho, and B. Lee, "Wide-viewing-angle 3D/2D convertible display system using two display devices and a lens array," *Opt. Express* **13**(21), 8424–8432 (2005).
2. T. Dekker, S. T. de Zwart, O. H. Willemsen, M. G. H. Hiddink, and W. L. IJzerman, "2D/3D switchable displays," *Proc. SPIE* **6135**, 61350K, 61350K-11 (2006).
3. J. Flack, J. Harrold, and J. Woodgate, "A prototype 3D mobile phone equipped with a next generation autostereoscopic display," *Proc. SPIE* **6490**, 64900M (2007).
4. M. P. C. M. Krijn, S. T. de Zwart, D. K. G. de Boer, O. H. Willemsen, and M. Sluijter, "2D/3D displays based on switchable lenticulars," *J. SID* **16**(8), 847–855 (2008).
5. A. Takagi, T. Saishu, M. Kashiwagi, K. Taira, and Y. Hirayama, "Autostereoscopic partial 2-D/3-D switchable display using liquid-crystal gradient index lens," *SID Symp. Dig.* **41**, 436–439 (2010).
6. G. J. Woodgate, J. Harrold, A. M. S. Jacobs, R. R. Moseley, and D. Ezra, "Flat panel autostereoscopic displays-characterization and enhancement," *Proc. SPIE* **3957**, 153–164 (2000).
7. J. G. Lu, X. F. Sun, Y. Song, and H. P. D. Shieh, "2-D/3-D switchable display by Fresnel-type LC lens," *J. Disp. Technol.* **7**(4), 215–219 (2011).
8. R.-Y. Tsai, C.-H. Tsai, K. Lee, C.-L. Wu, L.-C. D. Lin, K.-C. Huang, W.-L. Hsu, C.-S. Wu, C.-F. Lu, J.-C. Yang, and Y.-C. Chen, "Challenge of 3D LCD displays," *Proc. SPIE* **7329**, 732903, 732903-8 (2009).
9. N. S. Holliman, N. A. Dodgson, G. E. Favalora, and L. Pockett, "Three-dimensional displays: A review and applications analysis," *IEEE Trans. Broadcast* **57**(2), 362–371 (2011).
10. L. G. Commander, S. E. Day, and D. R. Selviah, "Variable focal length microlenses," *Opt. Commun.* **177**(1-6), 157–170 (2000).
11. Y.-H. Fan, H. Ren, X. Liang, H. Wang, and S.-T. Wu, "Liquid crystal microlens arrays with switchable positive and negative focal lengths," *J. Disp. Technol.* **1**(1), 151–156 (2005).
12. Y. J. Liu, X. W. Sun, and Q. Wang, "A focus-switchable lens made of polymer-liquid crystal composite," *J. Cryst. Growth* **288**(1), 192–194 (2006).
13. Y. P. Huang, L. Y. Liao, and C. W. Chen, "2-D/3-D switchable autostereoscopic display with multi-electrically driven liquid-crystal (MeD-LC) lenses," *J. Soc. Inf. Disp.* **18**(9), 642–646 (2010).
14. Y. Liu, H. Ren, S. Xu, Y. Chen, L. Rao, T. Ishinabe, and S.-T. Wu, "Adaptive focus integral image system design based on fast-response liquid crystal microlens," *J. Disp. Technol.* **7**(12), 674–678 (2011).
15. J.-H. Na, S.-C. Park, S.-U. Kim, Y. Choi, and S.-D. Lee, "Physical mechanism for flat-to-lenticular lens conversion in homogeneous liquid crystal cell with periodically undulated electrode," *Opt. Express* **20**(2), 864–869 (2012).

16. E. Lueder, *3D Displays* (Wiley, 2012).
 17. Y.-J. Lee, J.-H. Baek, Y. Kim, J.-U. Heo, Y.-K. Moon, J. S. Gwag, C.-J. Yu, and J.-H. Kim, "Polarizer-free liquid crystal display with electrically switchable microlens array," *Opt. Express* **21**(1), 129–134 (2013).
 18. M. Schadt and W. Helfrich, "Voltage-dependent optical activity of a twisted nematic liquid crystal," *Appl. Phys. Lett.* **18**(4), 127–128 (1971).
 19. S. Xu, H. Ren, Y. J. Lin, M. G. J. Moharam, S. T. Wu, and N. Tabiryan, "Adaptive liquid lens actuated by photo-polymer," *Opt. Express* **17**(20), 17590–17595 (2009).
 20. H. Ren, Y.-H. Lin, and S.-T. Wu, "Flat polymeric microlens array," *Opt. Commun.* **261**(2), 296–299 (2006).
 21. N. S. Holliman, "3D display systems," in *Handbook of optoelectronics*, J.P. Dakin and R. G. W. Brown (Taylor & Francis, 2006).
 22. A. Naumov, G. Love, M. Y. Loktev, and F. Vladimirov, "Control optimization of spherical modal liquid crystal lenses," *Opt. Express* **4**(9), 344–352 (1999).
-

1. Introduction

Electrically switchable two-dimensional (2D) and three-dimensional (3D) displays have attracted great attention lately [1–7]. Each mode has its own unique merits. For examples, the 2D mode has wide view, high contrast ratio, and full resolution. When the 2D display is switched to 3D, the sense of depth appears and the images look natural. To convert a display between 2D and 3D modes, two main approaches have been proposed: 1) liquid crystal (LC) parallax barrier [3, 8, 9], and 2) LC lenticular microlens array [7, 10–15]. The former is simple to fabricate and easy to operate. However, its optical throughput is reduced to 50% because it is comprised of alternate transmissive and opaque columns aligned with the LC pixels. Compared to parallax barrier, LC lenticular microlens array offers high transmittance. Thus, it has been widely employed for switchable 2D/3D displays. For 2D display, the LC microlens has no optical power and it functions as an optically isotropic flat plate. To achieve 3D display, each microlens in the array should have optical power.

A lens whose focal length can be switched from a focusing state to non-focusing state is called switchable lens. Various switchable microlenses have been demonstrated [10–17]. To achieve a high focusing power, the optical path length difference ($d\delta n$) between the lens center and boarder should be large; here d is LC layer thickness and δn the LC refractive index difference. To enlarge $d\delta n$, we can increase d or use a high birefringence (Δn) LC. For a given LC material, increasing d would lead to a slow response time (proportional to d^2) and high operating voltage. To obtain a large gradient refractive index distribution or to shorten LC response time, often a complicate driving scheme is required. To overcome these issues, a twisted-nematic (TN) LC cell (or called polarization converter) [18,19] was proposed to indirectly actuate the LC lens [3]. Using the TN cell to control the polarization direction of the incident light, the LC lens could provide a switchable focus. This approach is intriguing because the LC lens can provide a switchable focus without actuation. However, both LC lens and TN cell require two glass substrates. So in total these two cells need four glass substrates. Undoubtedly, such an integrated lens system is bulky and heavy.

In this paper, we demonstrate the fabrication procedures of a static flat polymeric lenticular microlens array. When integrated with a dynamic TN polarization rotator, the static polymeric film becomes a switchable lenticular microlens array. It exhibits focusing and non-focusing states, depending on the incoming polarization. In this lens system, the TN cell is responsible for the dynamic switching, which is known to have a low operation voltage and reasonably fast response time. The fabrication procedure of the flat polymeric lens will be described in detail and the performance of the switchable microlens characterized. Its potential application for switchable 2D/3D display is emphasized.

2. Switchable 2D/3D display

Figure 1 depicts the device structure and operation principle of a switchable 2D/3D display based on the proposed static lenticular microlens array and a broadband TN polarization rotator. The structure consists of a 2D LCD panel (pixels), output polarizer, a TN cell, and a LC microlens array. Each LC microlens in the array covers two pixels: left and right. An

isotropic polymer with a concave shape is used as the base for the LC microlens array. Let us assume that the refractive index (n_p) of the isotropic polymer matches the ordinary refractive index (n_o) of the LC material. The LC in the lens cell presents homogeneous alignment. The optical axis of the polarizer is parallel to the rubbing direction of the bottom TN cell. In the voltage-off state ($V = 0$), the linearly polarized light passing through the polarizer is rotated 90° by the TN cell to be orthogonal to the LC directors in the lens cell. As a result, this ordinary ray will not be focused because $n_p \sim n_o$. The images from the left pixel and the right pixel can be seen by the two eyes at the same time. Therefore, the display remains the original 2D display [Fig. 1(a)]. When a high voltage is applied to the TN cell, the LC directors are reoriented along the electric field direction and the polarization rotation effect vanishes. The outgoing light from the TN cell behaves like an extraordinary ray to the lens cell. Because $n_e > n_p$ and the convex shape of the LC microlens, the focusing effect takes place. For each microlens, the image coming from the right pixel can only be seen by the left eye, while the image from the left pixel can only be detected by the right eye [Fig. 1(b)]. By combining these two images, our eyes will see 3D images out of the 2D panel.

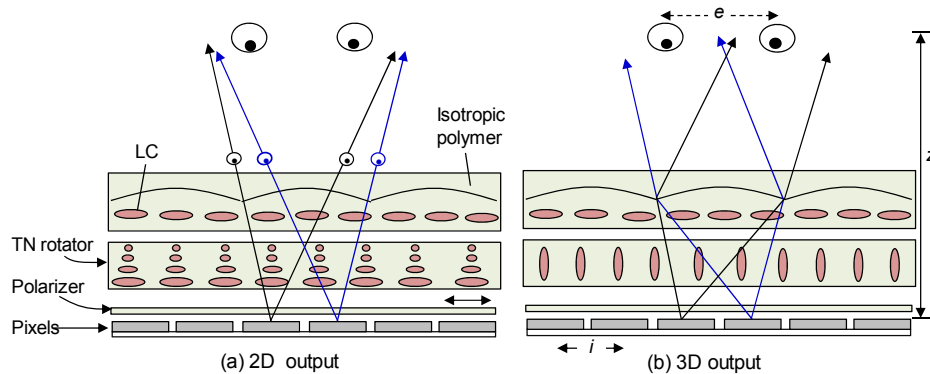


Fig. 1. Operation principle of a switchable 2D/3D display with a TN broadband polarization rotator (middle) and a polymeric microlens array (top): (a) voltage-off and (b) voltage-on.

From Fig. 1, the LC lens cell needs two glass substrates to hold the LC material. Together with the TN cell, four glass substrates are required, which is too bulky and heavy. Since the LC lens is not actuated during mode conversion, we can replace it with a lightweight polymeric lens without compromising its performance. Unlike a LC lens, the focal length of a solidified polymeric lens is insensitive to the surrounding temperature change.

3. Fabrication of polymeric lens array

To fabricate the abovementioned polymeric microlens array, we chose a diacrylate LC monomer because it is highly ordered and polymerizable. To obtain a lens-like gradient refractive index distribution, we need to generate an inhomogeneous electric field. The fabrication procedures of a flat polymeric lens are schematically illustrated in Fig. 2. In the mesogenic phase the diacrylate LC monomers are aligned in a homogeneous cell [Fig. 2(a)]. The ITO (indium-tin-oxide) electrode on the top substrate is continuous, but has a stripe pattern on the bottom substrate. Both substrate surfaces are over-coated with a polyimide (PI) alignment layer. The two PI layers are buffed in anti-parallel directions.

As Fig. 2(b) depicts, when a voltage is applied between the top common electrode and bottom stripe electrodes (all the stripe electrodes have equal potential), the LC monomers are reoriented. Above stripe electrodes, the longitudinal fields align the LC monomers in vertical direction. Between stripe electrodes, the superimposed fields have both vertical and horizontal components, and the resultant fields are shown by the red lines in Fig. 2(b). Because this fringing field is symmetric but inhomogeneous, a gradient refractive index

distribution is generated in the monomer bulk. After UV exposure [Fig. 2(c)], the monomers are solidified and the gradient refractive index distribution fixed. Next step is to remove the voltage and peel off the polymeric microlens array from the substrate [Fig. 2(d)]. Such a polymeric lens is thin and lightweight. Different from a circular polymeric lens which uses a hole electrode [20], here we use stripe electrodes to make a lenticular microlens array. By optimizing the electric field distribution, each lenticular microlens can offer a large gradient refractive index distribution without disclination defects.

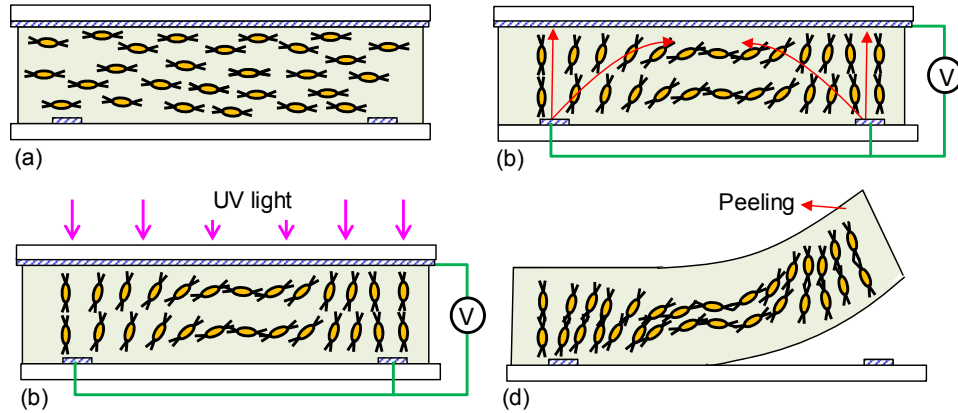


Fig. 2. Procedures for fabricating a polymeric lens: (a) homogeneous alignment of a diacrylate LC monomer at voltage-off state, (b) symmetric but inhomogeneous alignment at a voltage-on state, (c) UV curing to stabilize the molecular structure, and (d) peeling off the flat polymeric lens from the substrates.

4. Experiment

To fabricate a polymeric microlens array as shown in Fig. 2(d), we doped a diacrylate LC monomer RM 257 (Merck) with 1 wt% photoinitiator (benzophenone). RM257 with reactive double bonds at both sides has rod-like structure, which exhibits nematic phase from 70 °C to 130 J°C. Similar to a nematic LC, RM257 can also be aligned in a homogeneous cell. The ordinary and extraordinary refractive indices of RM 257 are $n_o = 1.508$ and $n_e = 1.687$, and dielectric anisotropy $\Delta\epsilon = -1.5$. In order to reorient the monomers along the electric field direction, we need a positive $\Delta\epsilon$. Thus, we mixed ~20 wt% Merck BL038 ($\Delta n = 0.272$, $n_o = 1.527$, $\Delta\epsilon = 16.9$) with RM257. The transition temperature of the mixture from nematic phase to isotropic phase was measured to be ~125°C. The blended RM257/BL038 mixture has three desirable features at room temperature: (1) positive $\Delta\epsilon$ (~ + 2); (2) $\Delta n \sim 0.197$ and (3) a better flexibility after UV curing. The mixture was thoroughly stirred at ~75 °C and injected into a homogeneous cell by capillary flow. The cell was then kept at this temperature for 2 minutes. so that the monomers could also be aligned by the rubbed polyimide layers. The cell gap, ITO stripe, and gap between ITO stripes is ~50, 20, and 100 μm , respectively.

To realize a broadband polarization rotator, we filled a TN cell ($d \sim 5 \mu\text{m}$) with a nematic LC mixture P0616A ($n_o = 1.521$, $\Delta n = 0.199$, $T_c = 58 \text{ }^\circ\text{C}$, Chengzhi Yonghua Display Material, China). According to Mauguin condition, our cell satisfies the relationship of $d\Delta n \gg \lambda/2$ in the visible region so that our TN cell is a broadband polarization rotator. It can rotate the polarization plane of a linearly polarized light by 90°.

5. Results and discussion

Before UV exposure, we evaluated the alignment of the lens cell in the voltage-off state using a polarizing optical microscope (POM). The cell was placed between two crossed polarizers. Initially the temperature of the cell was controlled at ~75 °C. When we rotated the cell on the stage, we observed alternating dark and bright states. When the cell rubbing direction was

parallel to the optical axis of the polarizer, a dark state was observed [Fig. 3(a)]. The short and bright lines are the defect orientation of monomers caused by the glass spacers. Rotating the cell by 45° led to a bright state [Fig. 3(b)]. These results indicate that the RM257/BL038 mixture is aligned well although the cell gap is fairly thick ($\sim 50 \mu\text{m}$). To study the temperature effect on monomer alignment, we deliberately decreased the temperature of the cell. Figure 3(c) shows the alignment of the cell as the temperature is decreased to 65°C for 1 minute. At 65°C , RM257 is crystallized and butterfly-like defects emerge. After 2 minutes the dimension of the defects grows [Fig. 3(d)], which eventually deteriorates the monomer alignment. Therefore, we need to control the temperature in the nematic range of RM257/BL038 in order to obtain homogeneous alignment.

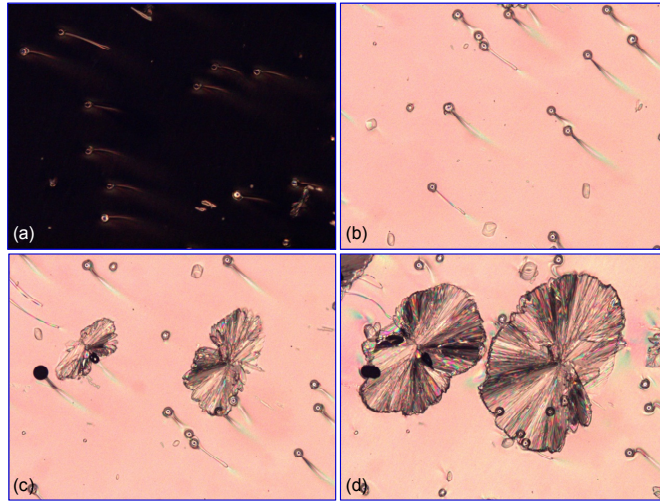


Fig. 3. Alignment of the monomer/LC cell at different conditions: (a) at 75°C with rubbing direction along the optic axis of a polarizer, (b) at 75°C with rubbing direction oriented at 45° to the axis of one polarizer, (c) at 65°C for one minute and (d) at 65°C for two minutes.

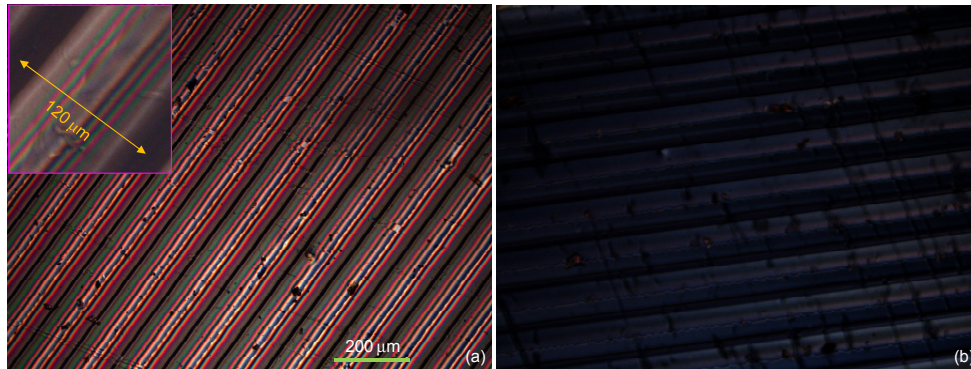


Fig. 4. The POM images of UV cured RM257/BL038 cell: the rubbing direction is (a) 45° and (b) 0° to the optical axis of the polarizer.

Before UV exposure, the temperature of the cell was controlled at $\sim 75^\circ\text{C}$ for several minutes. Under this temperature, the anisotropic dielectric of mixture $\Delta\epsilon$ was measured to be ~ 0.065 at 1kHz (HIOKI 3532-50 LCR HITESTER). Next, we applied $50 \text{ V}_{\text{rms}}$ (1 kHz) to the cell. Immediately the RM257/BL038 mixture was reoriented by the generated fringing fields [Fig. 2(b)]. The cell was then cured using UV light so that the monomers were polymerized. The UV light intensity was $\sim 20 \text{ mW/cm}^2$ and the exposure time was ~ 5 min. After polymerization, the voltage was removed and the cell was cooled down to the room

temperature. To inspect how the electric field affects the orientation of the formed polymer, we observed the birefringence colors under POM. The cell was placed on the microscope stage between crossed polarizers. The rubbing direction of the cell was oriented at 45° with respect to the transmission axis of the polarizer. Figure 4(a) shows the observed interference color which has a periodic stripe patterns. The color stripes between adjacent black lines (ITO stripes) imply that the polymer presents a gradient refractive index distribution. In each period, the solidified polymer exhibits lenticular lens characteristics. So the cell functions as a lenticular microlens array. The insert is the enlarged texture of one period, and the lens aperture is $120\ \mu\text{m}$. The tiny black spots in Fig. 4(a) are the defects which present the butterfly-like structure shown in Fig. 3(d). Because the temperature of the cell is slightly higher than the phase transition temperature of the monomer (from nematic to crystal phase), when the cell is transferred from the hot plate to the stage of the microscope, some domains in the mixture become crystallized as the temperature decreases. To minimize the defects, a constant temperature is important during the preparation of polymeric lens, and a temperature controller should be taken into account in future. The cell was then rotated by another 45° so that its rubbing direction is parallel to the optical axis of polarizer. A very dark state is observed [Fig. 4(b)] indicating that the polymeric microlens is indeed optically anisotropic. Its optical axis is along the rubbing direction of the cell.

To peel off the polymeric film, we kept the substrate at an elevated temperature. The film is flat and flexible, and can be easily handled using a tweezers [Fig. 5(a)]. The size of the film is $40\ \text{mm} \times 40\ \text{mm}$. To evaluate the quality of the microlens array after peeling, we observed the film under POM. Figures 5(b) shows a photo with polymer film's axis oriented at 45° to the optical axis of the polarizer, and the insert shows the enlarged texture of one period. It keeps the periodical interference color pattern as that of the original film sandwiched between two glass substrates. As Fig. 5(b) shows, some microlens axes were found to be slightly distorted, which may result from the electro-static force during peeling and lamination. When the optical axis of the film is parallel to the polarizer's axis, a very good dark state is observed [Fig. 5(c)]. It further indicates the film preserves the same performance as that of the original film. By removing the analyzer and adjusting the distance between the eyepiece and the sample, we can observe shape focal lines, as shown in Fig. 5(d). The bright lines imply that the microlenses are positive. The semi-bright lines are the light leakage above the stripe electrodes. To improve the lens performance, it would be better to use a black electrode (chromium) to replace the ITO electrode or block the ITO electrode with an opaque material. The focal length of the lenticular microlens was measured to be $\sim 0.65\ \text{mm}$. Therefore, the effective birefringence of our mixture is estimated to be $\delta n \sim 0.06$ at 75°C , which can be further increased after optimizing the device structure (e.g. electrode width, electrode gap, cell gap).

The impact of temperature on the focal length change by was also studied by observing the interference stripes as well as the color of the film. As the temperature decreased from 60°C to 23°C , no obvious change was observed. Such a result implies that the focal length is quite insensitive to the temperature change. The reasons are explained as follows: (1) Our LC/monomer mixture contains 80 wt% RM-257 and 20 wt% nematic LC BL-038. The mixture shows no phase separation after UV exposure. The LC molecules in the polymer are aligned well in the polymer film. The clearing point for RM-257, BL-038 and RM/LC mixture is 128°C , 100°C and 125°C , respectively. The birefringence of an LC depends on the order parameter of the LC system, which in turn depends on the reduced temperature (T/T_c). Therefore, high clearing point plays an important role in making the birefringence insensitive to the temperature variation, especially from 23°C to 60°C (a typical operation temperature range for an LCD). (2) The LC/monomer mixture was UV cured, so their structure is further stabilized. As a result, their birefringence is not sensitive to the temperature, provided that the temperature is way below T_c . Therefore, the performance of

our polymeric lens will not degrade as the surrounding temperature of the 3D display changes.

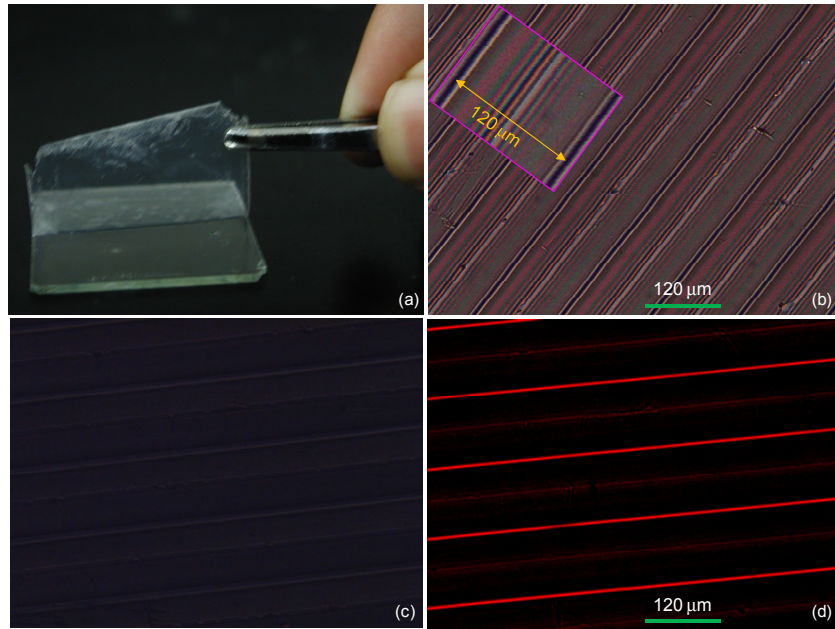


Fig. 5. (a) Photo of the solidified film during peeling, (b) image of a film observed under POM with its axis oriented at 45° and (c) 0° to the axis of the polarizer, and (d) in focused state with a red color filter.

The phase profiles of one microlens across its aperture before and after the lamination process were also calculated. The results are shown in Fig. 6. The phase profile is due to the refractive index change of the polymer and LC in the solid film. The two curves are overlapped well and they present parabolic shape.

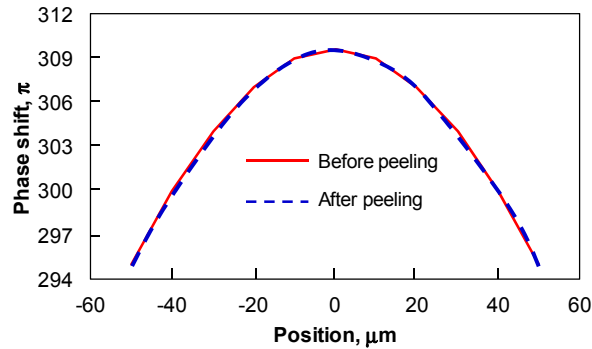


Fig. 6. The phase profiles of one polymeric microlens before and after peeling.

Since ~20 wt% LC was mixed in the polymeric film, it is important to evaluate the formed morphology of the film after peeling. One convenient way is to use scanning electron microscope (SEM) to detect the surface topography of the polymeric film. Figure 7(a) shows the image of the film surface morphology (magnification 25,000X). The surface of the polymeric film is very smooth except some isolated cavities. The average size of the cavities is ~30 nm. These tiny cavities should be the places occupied by the LC. Due to the crossed linking of the monomers after polymerization, the nano-sized LC domains are tightly sealed

in the film bulk. Cross-sectional morphology of the film was also observed, as shown in Fig. 7(b) (magnification 1,000X). No big LC domains are observed in the bulk. Because the domain sizes are so small, the film does not scatter light.

To switch the polymeric microlens between a focusing and non-focusing states, we integrated the film with the prepared TN cell. The setup for evaluation is shown in Fig. 8(a). A collimated linearly-polarized He-Ne laser beam ($\lambda = 633$ nm) illuminated the TNLC cell and the polymeric film. After passing through an imaging lens and an iris diaphragm, the laser beam was detected by a CCD camera (SBIG model ST-2000XM). The polarization direction of the beam is parallel to the front rubbing direction of the TNLC cell, and perpendicular to the optical axis of the polymer film, as shown by the pointed arrows. The TN cell was driven by a computer-controlled LabVIEW data acquisition system. The distance between the polymeric lens and the imaging lens was adjusted until the clearest image was observed on CCD. Because the polarization direction of the laser beam after passing through the TN cell is rotated 90° , it can be focused by the polymeric film.

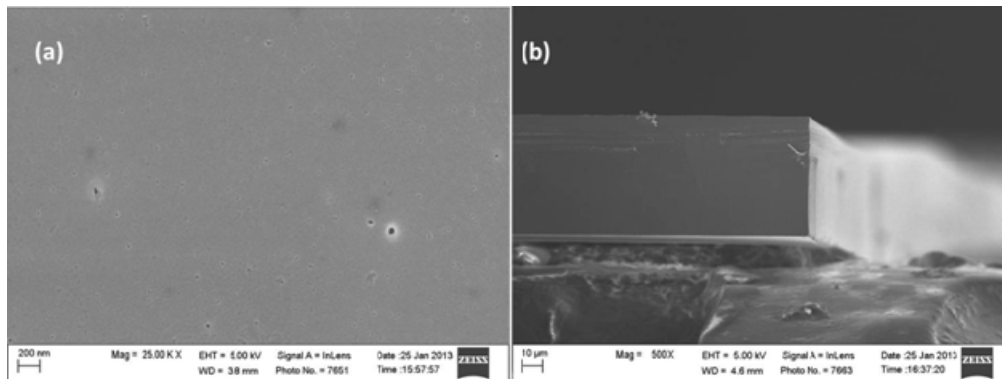


Fig. 7. SEM images of the polymeric film: (a) surface morphology and (b) cross-sectional morphology.

Similar to the results in Fig. 5(b), parallel focused lines are clearly observed. Figure 8(b) shows five focused lines of the beam (left) by the polymeric microlens array. A small background noise is observed as well. Since the lens is not perfect and a laser beam is used as the light source, interference and diffraction are responsible for the noise. The CCD intensity profiles across seven lines are also given in the right side of Fig. 8(b). The measured intensity of each focused line exceeds:64,000 arbitrary units and is quite uniform. When a voltage of $10 V_{\text{rms}}$ (1 kHz) is applied to the TN cell, the LC directors are reoriented along the electric field. As we explained in Fig. 1, the polymeric film presents uniform refractive index to the ordinary ray. Figure 8(c) shows the image of the beam passing through the polymeric film (left). No residual focusing effect is observed except the blurry tracks of the original focused lines. The output intensity is relatively uniform and its average intensity reaches:18000 arbitrary units. Comparing the results shown in Figs. 8(b) and 8(c), we find that our polymeric lens has a switchable focus by controlling the input polarization state through the TN cell. Similar to a conventional TN device, our TNLC/polymeric lens can be switched with a low driving voltage. Using a photodiode to replace the CCD camera, the switching speed could be measured easily. By adjusting the aperture of the diaphragm (Fig. 8(a)), the photodiode would detect higher light intensity in the focusing state and lower intensity in non-focusing state. Under a $10 V_{\text{rms}}$ pulse, the time from focus (non-focus) to non-focus (focus) was measured to be ~ 12 (~ 40) ms. In comparison to previous switchable LC lenses, our integrated TN/polymeric lens exhibits fast response time and low operating voltage, while keeping compactness and lightweight. The response time can be further reduced by using a low viscosity LC mixture.

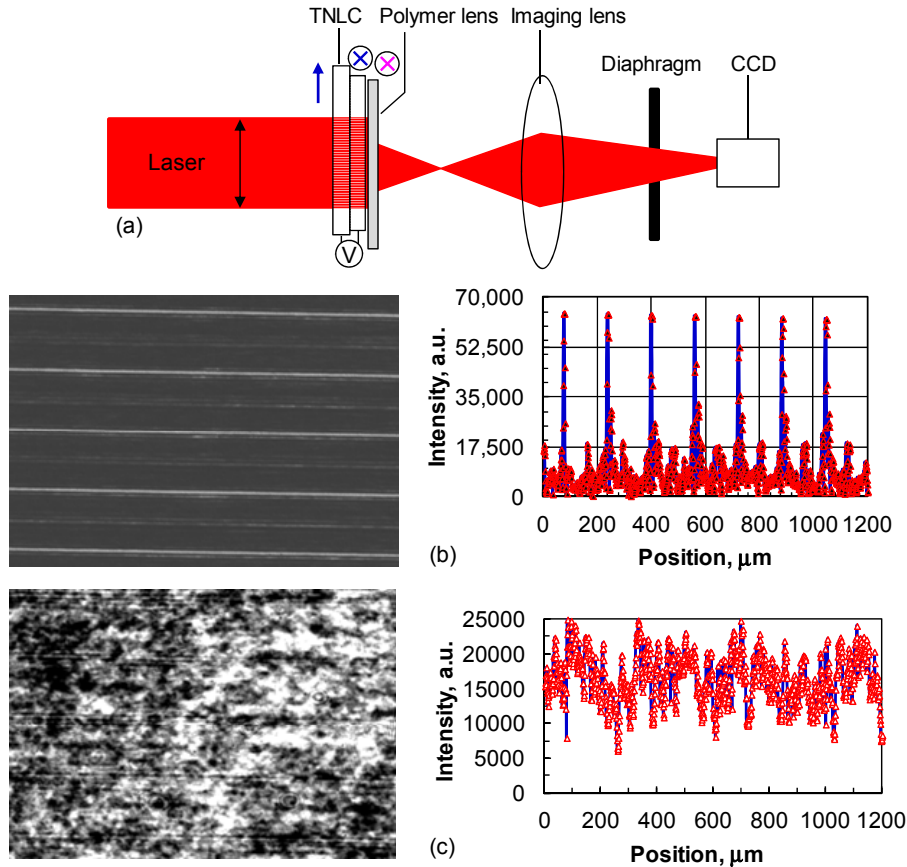


Fig. 8. Evaluation of the focus switching of the TNLC/polymeric lens: (a) Experimental setup, (b) imaging and intensity profiles of the focusing state, (c) imaging and intensity profiles of the non-focusing state.

From our microlens array, the lens aperture is $120\ \mu\text{m}$ and the measured focal length is $f \sim 0.65\ \text{mm}$, so the lens only yields $\sim f/5$. The f-number is determined by the lens aperture and focal length. Generally speaking, for 2D/3D switchable display application, the lens aperture depends on how many pixels to be covered by each lens, and the focal length depends on the pixel pitch, observation distance, and pupil distance, *etc.* In a typical 3D display, the relationship between the minimum focal length (f) of the microlens, the pixel pitch (i), the observation distance (z) and the pupil distance (e) [(Fig. 1(b))] can be expressed by [21]

$$z = f \left(\frac{e}{i} + 1 \right) \quad (1)$$

Typically the window width for the left eye and right eye is made to be the average pupil distance, in order to allow some freedom of movement around the nominal viewing position. For the fixed average pupil distance and the pixel pitch, a short distance z will require a short focal length accordingly. For cell phone application as an example, if $z = 250\ \text{mm}$, $i = 85\ \mu\text{m}$, and $e = 65\ \text{mm}$, then the focal length f is calculated to be $\sim 0.32\ \text{mm}$. Like other lenticular LC lens, the focal length of our lens can be controlled by an external voltage before UV exposure. The focal length of the lens is expressed as [22]

$$f = \frac{\pi w^2}{(4\Delta\phi\lambda)} \quad (2)$$

where w is the width of the lenticular lens aperture, $\Delta\phi$ is the phase retardation measured from the lens center and edge, and λ is the light wavelength. For a given w and λ , to get a short focal length we should increase $\Delta\phi$. To achieve a large $\Delta\phi$, we could optimize the cell structure in order to generate steep fringing field to create a large gradient refractive index profile.

To get a large size polymeric lenticular microlens array, a flexible substrate is highly desired, since it can be easily peeled off from the solidified polymeric film without any damage. Based on our approach, the polymeric film can be made like a paper; it can be easily installed on a conventional liquid crystal display for 3D imaging or removed for 2D imaging. In this way, the TN cell is no longer required. Our polymeric microlens array allows a switchable 2D/3D displays without the concerns of bulkiness and fragility.

6. Conclusion

We have demonstrated a flat polymeric microlens array for switchable 2D/3D displays. Under a fringing field, a gradient refractive index distribution can be induced within homogeneous aligned LC diacrylate monomers. After UV curing, the monomers form a polymeric film with a lens-like characteristic. The film is optically anisotropic and flexible, and can stand without any substrate. Integrating with a 90° TNLC cell, the lens behavior can be switched between a focusing state and non-focusing state. The entire system is as compact as other switchable LC lenses but has a lower operating voltage and faster response time. The lens performances can be further improved by optimizing the device structure and choosing proper materials. Various flat polymeric lenticular microlenses can be prepared through our approach. They are promising for switchable 2D/3D displays applications.

Acknowledgments

H. Ren is supported from the National Research Foundation (NRF) of Korea, the Korea-China Joint Research Program (2012-0004814). The University of Central Florida group is indebted to the U.S. Air Force Office of Scientific Research (AFOSR) for partial financial support under contract No. FA95550-09-1-0170.